

---

**INDC**

---

---

**INTERNATIONAL NUCLEAR DATA COMMITTEE**

---

A STATUS REPORT ON NUCLEAR DATA

FOR SHIELDING CALCULATIONS

C. Dunford\*, F. Fröhner\*\*, R.J. Howerton\*\*\*,  
O. Ozer\*\*\*\*, J.J. Schmidt\*, S. Valente\*\*

(Presented at the 4th International Conference  
on Reactor Shielding, Paris, October 9-13, 1972)

- \* Nuclear Data Section, Division of Research and Laboratories,  
International Atomic Energy Agency
- \*\* Centre de Compilation de Données Neutroniques, Saclay,  
France, Nuclear Energy Agency of the OECD
- \*\*\* Lawrence Livermore Laboratory, Livermore, California, USA
- \*\*\*\* National Neutron Cross Section Center, Brookhaven National  
Laboratory, Upton, New York, USA

29 March 1973

To: Recipients of INDC(NDS)-48/G

Subject: Corrections.

First, on page 4, the synthesis of photon interaction cross sections from LLL and NBS evaluations was done by John Terrell and Ernie Plechaty. The data were placed in the ENDF/B format by Mrs. Jean Graven.

Second, on page 18, the statement that most of the gamma production data in the ENDF/B library have been taken from the Livermore Library is incorrect. The only ENDF/B photon production data LLL has supplied to the ENDF/B Library is for Be<sup>9</sup>.

A STATUS REPORT ON NUCLEAR DATA  
FOR SHIELDING CALCULATIONS

C. Dunford\*, F. Fröhner\*\*, R.J. Howerton\*\*\*,  
O. Ozer\*\*\*\*, J.J. Schmidt\*, S. Valente\*\*

(Presented at the 4th International Conference  
on Reactor Shielding, Paris, October 9-12, 1972)

November 1972

- \* Nuclear Data Section, Division of Research and Laboratories,  
International Atomic Energy Agency
- \*\* Centre de Compilation de Données Neutroniques, Saclay,  
France, Nuclear Energy Agency of the OECD
- \*\*\* Lawrence Livermore Laboratory, Livermore, California, USA
- \*\*\*\* National Neutron Cross Section Center, Brookhaven National  
Laboratory, Upton, New York, USA

### Abstract

This paper first reviews the nuclear data requirements for shielding applications as contained in the most recent, first world-wide request list for reactor nuclear data measurements (RENDA 72). It then surveys the availability of neutron cross section and photon production data relevant to shielding in the major evaluated nuclear data libraries. A brief description of present and planned major evaluation efforts is given. Further information is presented on methods, both experimental and theoretical, for obtaining photon production data. The report concludes with a discussion of the present knowledge of the prompt fission neutron spectra.

### Resumé

Le rapport ci-joint donne une revue des données nucléaires nécessaires pour la protection des réacteurs en tant qu'exprimées dans la plus récente première liste mondiale des demandes de mesures des données nucléaires pour des réacteurs (RENDA 72). Il continue à décrire les sections efficaces neutroniques et les données pour la production des photons importantes pour la protection continues dans les bibliothèques les plus connues des données nucléaires évaluées. Ceci est suivi d'une brève explication des efforts plus importantes dans le domaine d'évaluation poursuivis à présent et pourvus pour la future. En plus information est présentée concernant les méthodes expérimentales et théoriques pour obtenir des données pour la production des photons. Le rapport se termine par une discussion de la connaissance contemporaine des spectres de neutrons prompts de la fission.

## I. Nuclear data requirements for shielding including neutron cross sections and gamma production data

The nuclear data requirements for shielding cover a variety of neutron cross sections and gamma production data for a rather broad range of nuclides. In the past this subject was reviewed particularly by Goldstein [1,2] with an additional emphasis on the importance of accurate microscopic data for shielding design. More recently great progress has been made in discrete ordinates and Monte Carlo methods as applied to shielding calculations allowing more accurate and detailed theoretical predictions of neutron and gamma ray fluxes, dose rates, etc., than previously [3]. This places an increasing stringency on the detail and accuracy with which the pertinent nuclear data have to be known.

Unlike for reactor core physics, only selected sensitivity studies have been performed so far regarding the detailed influence of nuclear data uncertainties on shielding design (see for instance [4]). Furthermore the results of more comprehensive sensitivity studies underway or planned, which are designed to give a more detailed picture of the actual accuracy needs in terms of design and economics penalties, must be considered before detailed requirements can be ascertained. Also it is not the purpose of this paper to go deeper into the question of nuclear data needs as this will form the subject of the subsequent panel at this Conference. It seems, however, adequate to outline briefly the present requirements and to confront them with the actual availability of the data in the greater evaluated nuclear data libraries in the next chapter.

The present requirements, although by far not comprehensive, are best illustrated by the nuclear data requests for shielding purposes as contained in the most recent and first world-wide edition of RENDATA, RENDATA 72 [5]. A summary of the requests is given in figure 1. Six groups of requests can be discerned:

- total cross sections;
- elastic scattering angular distributions;
- cross sections for neutron production by inelastic neutron scattering;
- cross sections for gamma ray production by inelastic neutron scattering;
- bulk neutron emission cross sections;
- bulk gamma ray production cross sections.

The accuracies of 1% in  $\sigma_T$  requested for Na and Ni are rather outside present experimental capability, particularly in the cross section minima. This problem is treated extensively in the paper by Fröhner and Valente [6] submitted to this conference.

Elastic scattering angular distributions are particularly requested in the MeV range above 5 MeV illustrating the difficulties of measurements due to the lack of appropriate neutron sources particularly in the range 8-14 MeV.

Measurements of bulk neutron and gamma ray production cross sections are given higher priority on the average than those of cross sections for neutron and gamma-ray production due to inelastic scattering alone, although (with the exception of fission reactions) inelastic scattering is generally the most prominent production process between the lowest threshold and the onset of the  $(n,2n)$  process due to the smallness of the capture cross section compared to the inelastic scattering cross section. The accuracies requested for these four types of reactions are rather modest and are generally well within reach of present experimental techniques. They emphasize again the MeV range of neutron energies as particularly important for shielding problems except for bulk gamma ray production, where gamma ray spectra created by neutron capture below the lowest inelastic scattering threshold are important.

Almost all of the mentioned RENDA 72 requests seem still to be concerned more with bulk shielding problems than with more specific shielding aspects such as (to mention only one example) the build-up of trans-uranium isotopes such as  $\text{Cm}^{242}$  and  $\text{Cm}^{244}$  in irradiated fuels which represent neutron sources through spontaneous fission and  $(\alpha,n)$  reactions and are thus of importance both for criticality control and the shielding of fuel-handling equipment including transport flasks [7,8]. It is hoped that the Study Group Meeting which the IAEA plans for the first half of 1974 will review in detail the nuclear data requirements for shielding particularly on the basis of comprehensive and detailed sensitivity studies so as to give the experimental efforts needed to fulfil these requirements a more precise and firm foundation.

## II. Shielding nuclear data content of the major evaluated nuclear data libraries

In this chapter we give an outline of the present content of the major evaluated nuclear data libraries, whereas chapters III and V will be reserved to a discussion of evaluation activities underway and planned and of evaluation methods of gamma-ray production cross sections respectively and chapter IV to integral nuclear data testing.

Figures 2 to 7 show schematically the contents of the three main files of evaluated neutron data for a series of elements with special importance for shielding and filter applications. The energy ranges in which evaluated data exist are given. In addition, the regions for which the files contain complete sets of resonance parameters are indicated in the total cross section diagram. The data types considered are the total, differential elastic scattering, radiative capture,  $(n,p)$  and  $(n,\alpha)$  cross-sections, inelastic neutron spectra and gamma production cross-sections.

Regarding the present status of ENDF/B it might be of interest to add that the formats described in the ENDF Formats and Procedures Manual (LA-4549 ENDF-102, Rev., Vol 2 July 1971) allow considerable detail in the representation of photon data since separate files are defined for:

- |  |           |
|--|-----------|
| a) Photon multiplicity and transition probability arrays | (file 12) |
| b) Photon production cross sections                      | (file 13) |
| c) Photon angular distributions                          | (file 14) |
| d) Continuous photon energy spectra                      | (file 15) |
| e) Photon energy-angle distributions                     | (file 16) |
| f) Photon interaction "smooth" cross sections            | (file 23) |
| g) Secondary angular distributions                       | (file 24) |
| h) Secondary energy distributions                        | (file 25) |
| i) Secondary energy-angle distributions                  | (file 26) |
| j) Atomic form factors or scattering functions           | (file 27) |

It has been the policy of the US Cross Section Evaluation Working Group (CSEWG) to supply evaluated cross sections in fine enough detail when such detail is considered useful. Thus in addition to the  $(n,n'\gamma)$  and  $(n,\gamma)$  cross sections given for all pertinent materials the ENDF/B version III library contains twelve complete evaluations with specifically shielding oriented photon files. All cross sections for these materials are supplied up to an upper energy limit of 20 MeV when applicable.

A list of these 12 materials as well as the type of data available for each is given in the table below.

<u>Element</u>	<u>MAT</u>	<u>Evaluator</u>	<u>Lab</u>	<u>file 12</u>	<u>file 13</u>	<u>file 14</u>	<u>file 15</u>	<u>file 23</u>
H-1	1148	L. Stewart et al.	LASL	X		X		
Se-9	1154	R.J. Howerton, S.T. Perkins	LLL		X	X		
N-14	1133	P.G. Young, D.G. Foster	LASL	X	X	X		
O-16	1134	P.G. Young, D.G. Foster	LASL	X	X	X		
Na-23	1156	Paik, Pitterle, Perey	WARD, ORNL	X		X	X	X
Al-27	1135	D.G. Foster, P.G. Young	LASL	X	X	X	X	
Si	1151	M.K. Drake	BNL, GGA	X	X	X	X	
Cl	1149	M.S. Allen, M.K. Drake	GGA	X	X	X	X	X
K	1150	M.K. Drake	GGA	X	X	X	X	X
Cu	1152	F. Perey, M.K. Drake	ORNL, GGA	X		X	X	X
Fe	1180	Penny, Kinney et al.	ORNL	X		X	X	X
Pb	1136	C.Y. Fu, F. Perey	ORNL	X		X	X	X

List of ENDF/B version-III materials with shielding data files.

In addition to the twelve materials listed in the above table the ENDF/B version-III library also contains a file of photon interaction cross sections (ENDF tape 330). This file consists of a combination of LLL and NBS tabulations placed into the ENDF/B format by R.J. Howerton. Eighty-seven materials, each corresponding to a separate element, are given. The data for each material consists of a short Hollerith description (file 1 section 451) and the following photon interaction types:

- |                          |                       |
|--------------------------|-----------------------|
| a) Total                 | (file 23 section 501) |
| b) Coherent scattering   | ( " " " 502)          |
| c) Incoherent scattering | ( " " " 504)          |
| d) Pair production       | ( " " " 515)          |
| e) Photo effect          | ( " " " 602)          |



In its present status the German nuclear data library MEDAK is mainly intended for fast reactor calculation purposes. So far no use has been made of it in reactor shielding calculations except for few test runs and comparative integral checks of neutron transmission. Therefore it will not provide a number of data types needed by current shielding codes to calculate the  $\gamma$  sources and  $\gamma$ -transport, esp.  $\gamma$ -production cross sections and secondary  $\gamma$  distributions. It contains, however, for a number of materials all data necessary to carry out the neutronic part of the shielding calculation [18-20].

Figures 2 through 7 indicate that there still exist serious gaps and deficiencies.

- With the exception of several materials in the ENDF/B file there exist no data on photon production spectra irrespective of the origin of the produced photons.
- The evaluated data libraries do not contain capture gamma ray spectra. To our knowledge evaluation efforts are at present only made for ENDF/B.
- Neutron inelastic excitation cross sections seem to be fairly well covered in all four libraries and either data or scattering laws provided for energy distributions of inelastically scattered neutrons in the continuum. For all other inelastic scattering and photoproduction data figure 7 shows still a number of gaps.
- None of the files contains data on barium, in spite of its importance as an admixture in concrete shields.
- None of the files contains cross section data for neutron energies above 15 MeV, although such data are needed for accelerator shielding.
- The UKNDL library does not give resonance parameters at all - and the others none for B, N, Si, Ca, Zr or Pb.

Other deficiencies are less obvious. For instance, none of the files contains error information (error bars, confidence limits). In fact, the uncertainties are often quite large. In many cases the evaluators had only sparse and inaccurate data to build on. Gaps had to be filled by means of more or less sophisticated theoretical estimates and interpolation procedures. Furthermore, each evaluation takes time, and experimental data are sometimes available long before they are incorporated in one of the evaluated files. The consequence is that evaluated data are often neither complete, nor up to date, nor is their accuracy known.

Users may therefore benefit from the non-evaluated experimental data files maintained at the neutron data centres, especially with regard to recent data or neutron energies above 15 MeV. For example total cross section data up to the GeV region exist for hydrogen, carbon, iron and lead as can be seen from the indexes published by the centres more or less regularly (see [9,10,11]).

Many of the difficulties encountered in shielding calculations with data from the evaluated files arise from the fact that these files were compiled originally for reactor core design rather than shielding applications. Only lately are the files being modified in order to make them more useful for shielding, deep-penetration and radiation transport work.

An illustrative example is provided by the problem of neutron windows. Most of these neutron windows - regions of very low total cross section - are in fact dips in the cross section due to interference between potential and resonance scattering particularly of light and medium-weight nuclei. Well known examples are the windows of oxygen at 2.35 MeV, of silicon at 55 and 144 keV, of scandium at 2 keV and of iron at 24.5 and 82 keV. These windows determine the neutron flux penetrating thick layers of the material - as for example demonstrated by Goldstein and coworkers for iron [14], and they can be used to produce practically monoenergetic neutrons by the filtered-beam technique [12].

Inspection of the evaluated and unevaluated neutron data files reveals that, with very rare exceptions, no good data on windows exist for reliable deep-penetration or filter calculations. One reason is again the fact that reactor core designers are generally most interested in the cross section peaks and much less in the valleys, so almost all total cross section measurements were performed with samples just thick enough to yield good accuracies for the resonance peaks and maybe the potential scattering cross section. Moreover, bad signal-to-noise ratio and counting statistics make accurate measurements in the window regions quite difficult. As a consequence, most of the data on windows are very inaccurate, sometimes only the order of magnitude of the minimum cross section is established.

In principle, window cross sections can be calculated from resonance parameters, but in practice the results of such calculations are frequently quite misleading. Reliable resonance parameters are normally available only for the s-wave part of the cross section. In pronounced neutron windows, however, the s-wave cross section drops to such low values - several orders of magnitude smaller than the potential-scattering cross section - that it becomes quite unimportant relative to contributions from p-, d-, ... wave cross sections and from impurities. The impurity contributions can often be calculated with adequate precision from evaluated cross section data or resonance parameters, but higher-

order partial wave contributions are usually unknown and must be estimated by means of level-statistical sampling methods or optical-model calculations (for more details see the contribution by F.H. Fröhner and S. Valente to this conference [6]).

The relative importance of these effects is shown by recent results obtained at the ORELA facility in Oak Ridge [13]. Using very thick and pure samples J.A. Harvey obtained data on 25 neutron windows in the total cross section of iron. He found for example a minimum cross section of 430 mb in the 24.5 keV window produced by an interference dip of  $\text{Fe}^{56}$ . About 305 mb are due to  $\text{Fe}^{54}$  (abundance 5.82 %), 110 mb due to  $\text{Fe}^{57}$  (abundance 2.19 %), and the rest comes from impurities of Cu and Mn (abundance 0.03 % for each) and from higher-order partial waves plus a mere 4 mb or so from the s-wave cross section of  $\text{Fe}^{56}$  (cf. also [6]).

The iron data in ENDF/B III were readjusted so as to agree with the empirical results in the 24.5 keV window, but not for the 24 other windows studied by Harvey. No other examples of similar measurements and readjustments are known to the authors.

Simplifying one can say that the needs of shielding specialists and of other users of total and scattering cross section data are complementary in the sense that shielders are mainly interested in the dips and other users in the peaks of the cross section. Presently available evaluated data correspond to the needs of other users much more than to those of the shielders. First steps are being taken to eliminate this mismatch with respect to shielding needs - the inclusion of data on neutron windows and of photon cross sections in the ENDF library is an encouraging example - but it will take a long time and much effort by data producers and evaluators until this goal will be achieved.

The construction of multigroup libraries for shielding purposes from microscopic neutron and photon production data is outside the scope of the present paper. However, it might be of interest to quote very briefly one typical example for these efforts which is provided by the shielding group at the Stuttgart University in Germany [15]. This group produces coupled neutron- and gamma production multigroup cross sections, at present in a standard version of 97 fast neutron groups, 1 thermal group and 18 gamma groups in  $P_5$ -approximation. Data in the thermal and epithermal ranges, where the field of secondary gammas depends particularly strongly upon the flux of thermal neutrons, are condensed, depending upon the actual problem treated, from a thermal 123 group cross section library with the inclusion of upward scattering.

In the USA the Radiation Shielding Information Center (RSIC) helps to meet the need for both computer codes and data libraries to solve radiation shielding problems. The activities of RSIC are more fully described in two papers being presented at this conference [16,17].

RSIC provides data libraries in two ways. In one arrangement, special data libraries are provided as part of computer code packages. These data libraries are apt to be in a special format that is not widely used by other computer programmes. Examples are the neutron energy point cross section library provided with CCC-17/05R, the multi-group cross section library provided with CCC-123/XSDRN, the gamma-ray production, the electron-photon cross section library with CCC-107/ETRAM, the multigroup neutron library with PSR-12/GGC and the activation cross section library with CCC-112/SAND II.

The other scheme is the assembly of data libraries which are packaged as separate units as part of the RSIC Data Library Collection (DLC). A list of the current DLC sets is given in another paper [17].

RSIC is the clearinghouse for the Defense Nuclear Agency (DNA) Working Cross Section Library [17]. The nature of the DNA library allows change at the evaluator's direction as often as indicated by new cross section measurements and other data testing results. For the materials sponsored under this programme, emphasis is placed on determination of cross section minima over the neutron energy range. The importance of neutron angular distributions at cross section minima is also stressed. Gamma-ray production for various neutron reactions is also recognized as important and attempts are made to determine them separately rather than combining all reaction cross sections into a single total gamma-ray production cross section. Since the DNA library is in ENDF format and is available for consideration by CSEWG to become part of the ENDF/B library, the DNA programme offers a good opportunity for improving the state of shielding cross sections.

The CSEWG Shielding Subcommittee is considering possible formats for handling time-dependent photon production data as well as resonance-dependent photon production data in anticipation of the need and importance of these types of data. RSIC is actively involved in these activities.

### III. Evaluation activities

In the Western hemisphere the main activities regarding nuclear data evaluation for shielding purposes are going on in the U.S.A. and U.K. These are briefly outlined in the following.

#### III.1 United States

The major activities in neutron evaluations for shielding applications in the United States are concentrated in the four laboratories given in the table below. The table also lists evaluations currently underway or planned. These evaluations are planned to be included as a part of the ENDF/B data library and many of them are expected to contain photon production data.

---

Los Alamos Scientific Laboratory P. Young	Li, B, N, O, Al, U <sup>238</sup>
---	-----------------------------------

---

Oak Ridge National Laboratory F. Perey	C, Ca, Fe, Ta, Pb
--	-------------------

---

Lawrence Livermore Laboratory R. Howerton	Many nuclides, photon production cross sections
---	--

---

Brookhaven National Laboratory M. Bhat A. Prince	Si, Cr, Co, Ni
---	----------------

---

Gulf Radiation Technology, M. Fricke	Mg, Co
Atomics International, E. Alter	W

---

NNCSC has been collecting and adapting a library of computer codes capable of calculating  $\gamma$ -production data from various neutron reactions and producing the output in ENDF format. (H. Takahashi, Gamma Ray Production Cross Sections of Neutron Induced U-238 Reactions, April 1972 report to the CSEWG Shielding Subcommittee). Already completed three independent evaluations of gamma production in U-238 (BNL, LASL and LLL) as well as the following evaluations in progress are expected to constitute the building blocks for the ENDF/B version-IV library.

AI: W isotopes  
BNL: Ni, Cr, Si  
GRT: Mg  
LASL: Li isotopes, B isotopes  
LLL: Ta, Be and others

(The above list does not include continuing updates of materials already listed on the table in chapter II.)

The usefulness of the ENDF/B library is expected to be further increased by the adoption of two new format modifications presently being considered. The first of these will allow for the time dependence of photons produced following the fission of a material to be given with the rest of the data for that material (as files 17 and 18). These format modifications will make calculations of fission product gamma ray production possible.

The second format modification will allow for specification of resonance dependent photon production data in order to treat more accurately cases where differential self shielding effects may be important.

The development of a computer code to process data in ENDF format and produce fluence-to-kerma factors was undertaken in a cooperative effort between RSIC and the University of Wisconsin Nuclear Engineering Program. The motivation was the need for this type of data in Controlled Thermonuclear Research neutronics studies. The result will be the computer code as well as a kerma factor library based on ENDF/B data with a handling programme to put the library in multigroup form.

The Oak Ridge National Laboratory has an extensive integrated experiment, theory, and evaluation programme under the direction of Dr. Francis Perey. The experimental work has been discussed briefly earlier in this paper and the theoretical work will be discussed in chapter IV of this report. A recent report from this evaluation group describes a complete evaluation including gamma ray production for lead [VI.2]. All the neutron induced reactions are evaluated simultaneously. Extensive use of theory and measurements is made. Nuclear structure data is evaluated and used for calculation of gamma-ray spectra and interpretation of experimental data.

The Los Alamos Scientific Laboratory group is also performing complete evaluations for shielding nuclides including photon production data. The National Neutron Cross Section Center (NNCSC) at Brookhaven National Laboratory is undertaking the task of collecting and adapting a library of computer codes capable of calculating  $\gamma$ -production data from various neutron reactions and producing the output in ENDF format. This activity is in addition to NNCSC activity in the neutron data evaluation field and its coordinating responsibility for ENDF/B. The group at the Lawrence Livermore Laboratory maintains an extensive file of measured and evaluated data with particular emphasis on shielding materials and the production of evaluated photon production libraries.

### III.2 United Kingdom

Shielding research and development in the United Kingdom has hitherto been largely concerned with the development of fast design methods, and shielding specialists have relied very much on their private data compilations which are methods-orientated and have been evolved as needs have arisen. Some compilations have been published however including those of gamma ray source spectra from neutron radiative capture and fission-product decay by E.W. Sidebotham at Risley, prepared as part of the data input for the programmes FISPEC and FISPIN.

As a result, shielding requirements have not figured prominently in the evolution of the UK Nuclear Data Library, and the satisfaction of data requirements for reactor core behaviour has been the predominant interest of the UKNDL evaluators. Nevertheless the UKNDL does contain photon scattering and attenuation cross-section data covering the energy range from 10 keV to 20 MeV for 26 materials from hydrogen to plutonium; see for example Norton (1968) AEEW-M 824.

An increasing degree of attention is being paid to "windows" in the neutron total cross-sections of low and medium weight materials, but mainly as a means of testing the choice of resonance parameter values and the completeness of the theory rather than in response to shielding requirements. For example, at the 24 keV minimum in the total cross-section of iron we find it very difficult to obtain a value much above 0.33 barns by calculation from resonance parameters, in conflict with recent measurements which suggest a value of about 0.50 barns. This discrepancy provides a caution against any early expectations for 1% accuracy (or even 10%) in measurements of cross-section minima by differential methods.

To provide comprehensive evaluations of gamma-ray production data for a wide range of materials and for a wide range of incident neutron energies would be a very large task: nor does the problem end there - computer files of evaluated data are of no use without associated processing programmes. Before embarking on a task of this nature it is very important for the shielding specialists to identify the sensitivity

of shield performance to nuclear data uncertainties, but the measurement of differential cross-sections to the accuracy indicated by these studies is not an automatic requirement. In fast reactor physics this line of argument led inevitably to high accuracy data requests which could not have been met in the time-scale required, whereas the combined use of integral measurements and differential data of lower accuracy has sufficed. A similar approach may very well be necessary for shielding assessments.

Having identified the data requirements through sensitivity studies, time scales and cost benefit should govern priorities and the proper balance between integral and differential measurements.



#### IV. Integral testing of evaluated neutron data for shielding

As an example for integral testing of evaluated neutron data for shielding a description is given below of a programme for measuring the time-of-flight spectra of neutrons emerging from thick spheres which has been carried out at the Lawrence Livermore Laboratory at Livermore in California. The spheres range in thickness from about 0.5 to about 5 mean free paths for 14 MeV neutrons. In these experiments a tritiated target is placed at the approximate center of a sphere of the material to be investigated, and a pulsed beam of deuterons is directed down a hole into the sphere and onto the target, producing 14 MeV neutrons. Neutron detectors are placed at angles of  $30^\circ$  and  $120^\circ$  with respect to the incident deuteron beam direction, at distances of approximately eight and ten meters, respectively. A complete description of the experiments and the resultant time spectra of detected neutrons is given in reference [23].

The pulsed sphere experiments were done in order to provide a mechanism for testing evaluated neutron data in the energy region from about 2 MeV to about 15 MeV. The spectra from thin spheres (0.5 to 1.5 mean free paths) provide a direct test of the accuracy of cross section evaluations in the 14 to 15 MeV energy regime, and the spectra from thicker spheres test the evaluated data over the full energy range from 2 to 15 MeV. In order to use the pulsed-sphere neutron time-of-flight spectra for testing evaluated neutron data, it is necessary to have a computer code that calculates an equivalent time spectrum. A simple energy spectrum calculation with multiple scattering effects included is not applicable for this purpose, since there is not a one to one correspondence between the arrival time of the neutron at the detector and the energy of the neutron. Monte Carlo neutronics codes can be modified relatively easily so as to produce calculated spectra which can be compared directly with the experimental spectra. The experimental spectra must be corrected for detector response functions, which are folded into the calculations. A very useful by-product of such calculations is the possibility of intercomparing Monte Carlo neutronics codes that use the same evaluated library for input. For example, several pulsed sphere time spectra were calculated at Lawrence Livermore Laboratory (LLL) and also at Los Alamos Scientific Laboratory (LASL), using the LLL evaluated data library and two different Monte Carlo neutronics codes. The LLL code uses 175 preselected neutron energies for input cross sections and does an analogue calculation, whereas the LASL code uses the cross section data in the pointwise form as provided by the evaluator and does an expectation calculation. The results of identical calculations done with the two codes agreed to within Monte Carlo statistics.

The main conclusion to be drawn from extensive calculations of pulsed sphere neutron time spectra is that a temperature model representation for scattered neutrons from  $(n,n'\gamma)$  reactions is totally inadequate for all materials with nuclear mass greater than 25 amu. Between five and ten percent of the emitted neutrons from nonelastic-

neutron-producing reactions are of higher energy than would be obtained from a temperature model, if reasonable nuclear temperatures are used. This 5 or 10 percent of all inelastic neutrons amounts to between 20 and 100 percent of the neutrons from just the  $(n,n'\gamma)$  reaction, depending on the relative magnitudes of the  $(n,n'\gamma)$ ,  $(n,2n)$  and  $(n,3n)$  reactions. Whether one subscribes to the "all direct-interaction" or "part direct-interaction, part pre-equilibrium" interpretation of this phenomenon, the fact remains that there are more high energy neutrons than can be accounted for by reasonable nuclear temperatures.

The pulsed sphere programme provides integral data to be used in testing evaluated neutron files for the adequacy of their representation of neutron-induced reactions in the energy range from 2 to 15 MeV. While it is obviously possible to force a "fit" to the experimental spectra by adjusting the evaluated data, it seems to be a much more useful approach to use the pulsed spheres only in a diagnostic role. That is, changes in the evaluated library should be made only if they can be justified by considerations that are apart from the fits to the pulsed sphere data. By using the pulsed spheres as this kind of an integral constraint, one can hope to gain an insight into the systematics of neutron emission spectra from high energy neutron-induced reactions.

## V. Experimental determination of photon production cross sections

Several facilities in four countries are presently being used to supply measurements of photon production cross sections and spectra. These facilities can be separated into two classes according to the method used to generate the source neutrons. This breakdown is given in the table below.

Electron linear (LINAC) accelerator	Oak Ridge National Laboratory Gulf Radiation Technology
Van de Graaff accelerator	Oak Ridge National Laboratory Obninsk Texas Nuclear Corporation Commissariat à l'Energie Atomique Kernforschungszentrum Karlsruhe Los Alamos Scientific Laboratory

To illustrate by a characteristic example the types of data generated by these two classes of facilities, the Oak Ridge programme which includes both LINAC [21] and Van de Graaff [22] measurements is described in the following:

The Van de Graaff accelerator system generates a beam of mono-energetic pulsed neutrons. This beam is incident on a right circular cylinder of the sample material (in this case Fe). The gamma rays produced in the neutron-target interaction are detected with a Ge(Li) detector placed at angles of 35, 55, 75, 90, and 125° relative to the incident neutron beam.  $\gamma$ -spectra were obtained for neutron energies between 5.35 and 9.0 Mev in half MeV intervals.

Fast-timing electronics is used to discriminate against most unwanted background events. Detector calibration, finite sample and multiple scattering corrections must be made. Corrections for self-absorption of gamma rays in a sample can become quite large for heavy nuclides like tantalum. The absolute calibration of the beam intensity is to an accuracy of about 7%.

A sample gamma spectrum at 125° for 4.85 Mev neutrons incident on natural iron is shown in figure 8. The shaded band indicates the underlying Compton distribution. In this figure an attempt has been made to identify the sources of all gamma rays observed. Absolute values of  $d\sigma/d\Omega$  can be obtained from the spectrum by

$$\frac{d\sigma}{d\Omega} = \frac{N_{\gamma}}{N_a N_b \Delta\Omega}$$

$N_{\gamma}$  = number of gamma rays detected

$N_a$  = number of atoms in the target

$N_b$  = neutron beam intensity

$\Delta\Omega$  = solid angle of the detector

The estimated error of the cross sections is less than 10% in most cases.

At the Oak Ridge Electron Linear Accelerator (ORELA) a Shield Test Station has been established for the measurement of gamma ray spectra. A general schematic of the experimental layout is shown in figure 9.

Neutrons are produced by photonuclear processes due to bremsstrahlung from electron impact on a tantalum target. The neutrons traverse a 47 meter flight path before striking the sample. Along the flight path is a Uranium 238 filter to reduce the gamma flash from the tantalum target, a boron-10 filter to remove all neutrons below 1 keV and a collimator. Approximately 40 meters of the flight path are under vacuum in order to increase the flux at the sample and reduce structure in the flux due to scattering resonances in air. At the target the beam has a diameter of about 10 cm and the energy profile is nearly constant across those 10 cm and known to about 10%.

A NaI crystal spectrometer assembly is used to detect the gamma rays emitted from the target at 125° from the incident beam. A shield of lead and lithiated paraffin surrounds the NaI detector to shield against unwanted neutrons and gamma rays. A lithium hydride slab is placed between the sample and the detector to eliminate scattered neutrons.

The pulse height signals from the NaI detector are stored by time-of-flight (that is the energy separation corresponding to the time the neutron requires to traverse the 47 meter flight path). The response of the NaI detector must be known in order to unfold the gamma-ray energy spectra from the pulse height data. This response function was determined by using calibrated  $\gamma$ -sources including radioactive isotopes such as  $^{137}\text{Cs}$ ,  $^{22}\text{Na}$ ,  $^{24}\text{Na}$  and a  $^{244}\text{Cm}$ - $^{13}\text{C}$   $\gamma$ -source. The response function was then tested with a known  $^{226}\text{Ra}$  source having at least 48 discrete gamma rays with well measured intensities.

Data were accumulated in 12 hour runs with alternating samples and background measurements. The background was obtained by inserting a lead bar between the sample and detector. A typical pulse height spectrum is shown in figure 10. An unfolded gamma-ray spectrum from iron is shown in figure 11. Note the numerous low intensity high energy gamma rays detected in this experiment due to fast neutron capture.

## VI. Evaluation of gamma ray production cross sections and spectra

Since gamma ray production cross sections and spectra available from measurements fill only a small part of the requirements for nuclear shielding calculations, it is necessary to use nuclear theory to fill in the information gaps. An evaluated data library for shielding calculations must contain information for all neutron incident energies, all possible reactions and for the emitted gamma ray spectra. At the present time there is no requirement for separate tabulations of gamma spectra from different reactions, only for a total gamma production cross section and spectrum. To illustrate the difficulties of the situation, consider the simple case where only the  $(n,\gamma)$  reaction produces photons. For thermal neutrons, one usually has measurements of the  $(n,\gamma)$  cross section, the photon spectrum, and the photon multiplicity. As the incident energy is increased and the resonance region is traversed, it is well known that the photon spectrum can and usually does change dramatically. For most materials, however, there are no measurements of the  $(n,\gamma)$  photon spectra and multiplicities other than at thermal neutron energies. Hence there is no experimental basis for including this changing photon spectrum. Above the  $(n,n'\gamma)$  threshold, most measurements are of specific photons and do not include the photon spectra from the  $(n,\gamma)$  reaction. Since the magnitude of the  $(n,\gamma)$  cross section is usually very small at these higher energies, photons from capture are lost in the background when the  $(n,n'\gamma)$  measurements are reported. Hence  $(n,n'\gamma)$  measurements do not help in determining the  $(n,\gamma)$  spectrum from high energy neutrons. Thus the problem remains of providing  $(n,\gamma)$  cross sections and spectra for neutron energies between about one ten-thousandth of an electron-volt and the threshold of the  $(n,n'\gamma)$  reaction (which is usually of the order of 10,000 electron-volts).

Two methods for generating gamma production data will be discussed here. The first method has been developed by Howerton and Plechaty [26] at the Lawrence Livermore Laboratory. This method has been extensively employed for the construction of the gamma ray production cross section portions of the Livermore Evaluated Neutron Data Library. Most of the gamma production data in the ENDF/B Library (USA) have been taken from the Livermore Library. This method is semi-empirical.

A second approach to the problem has been taken by the evaluation group (Fu and Perey [27]) at the Oak Ridge National Laboratory. Extensive use is made of the statistical model of the compound nucleus for the generation of detailed gamma spectra and gamma production cross sections. Gamma production data sets for Fe, Ta, and Pb which were generated by this method are now included in the ENDF/B Library.

# VI.1 Approach by Howerton and Plechaty [ 26 ]

The simplest nucleus, hydrogen, can be disposed of by noting that all the energy from neutron capture is emitted as a single photon, with energy

$$E_{\gamma}(\theta) = \frac{(Q+E_n)^2 + 2(Q+E_n)M_D C^2 - (E_n^2 + 2m_n E_n C^2)}{2(Q+E_n + M_D C^2 - \sqrt{E_n^2 + 2m_n E_n C^2} \cos \theta_{\gamma})}$$

where  $Q = 2.23$  MeV for  $H^1(n,\gamma)H^2$

$E_n$  = Incident neutron energy in the laboratory system

$M_D$  = Mass of the deuteron

$m_n$  = Mass of the neutron

$\theta_{\gamma}$  = Angle of the final state photon with respect to the incident neutron in the laboratory system.

At an incident neutron energy of 14 MeV, for example, we have

$$E_{\gamma}(\theta) = \frac{34556}{2(1910-163 \cos \theta_{\gamma})} \text{ [MeV]}$$

so that for  $\theta = 0^\circ$ ,  $E_{\gamma} = 9.9$  MeV, and for  $\theta = 180^\circ$ ,  $E_{\gamma} = 8.3$  MeV.

These calculated energies become more meaningful if one notes that the 14 MeV kinetic energy of the impinging neutron in the (n+p) laboratory frame of reference is approximately 7 MeV in the (n+p) center-of-mass frame of reference. The final state (D+γ) has center-of-mass and laboratory frames of reference that are essentially equivalent. Hence  $(\frac{E_n}{2} + Q)$  MeV is the available energy in both the center-of-mass and laboratory final state frames of reference. If an application requires a correlation of the photon energy with the incident neutron direction, then the equation above giving the energy-angle correlation is required. However, the simpler relation

$$E_{\gamma} \approx \frac{E_n}{2} + 2.23 \text{ [MeV]}$$

probably suffices for most applications. This gives a gamma ray energy that is halfway between the  $0^\circ$  and  $180^\circ$  values quoted above.

The above discussion of neutron capture in hydrogen is clearly a special, and in a sense a trivial case, although the same reasoning can be applied to the deuteron. However, the deuteron has an almost negligible cross section for neutron capture.

Turning to another problem involving light nuclei, one may consider neutron capture by  $\text{Be}^9$ . The only measurements are for thermal neutron capture, with multiplicities given for each detected photon. The Q-value for capture of a neutron by  $\text{Be}^9$  is 6.82 MeV, and at the (essentially zero) kinetic energy associated with thermal neutrons, about 40% of the photon production cross section is made up of the transition to the ground state, which yields a 6.82 MeV photon. The remainder of the photons are the result of cascades through the four levels of  $\text{Be}^{10}$  lying between the ground state and 6.82 MeV. As the incident neutron energy is increased, the energy of the primary ground state transition will be

$$E_{\gamma} \approx E_n \left( \frac{9}{9+1} \right) + 6.82 \text{ [MeV]}$$

For example, at 1 MeV the maximum photon energy will be 7.72 MeV. However, whether or not the direct transition remains at 40% of the total photon production cross section is completely unknown, and whether additional transitions occur through levels lying between 6.82 and 7.72 MeV in  $\text{Be}^{10}$  is not known, since the published level scheme for  $\text{Be}^{10}$  may or may not be complete in that energy regime. One is then faced with the problem of how to account for the extra available energy. In the absence of knowledge, the simplest assumptions are probably best, and in this case a useful assumption is to conserve the total energy adjusting the multiplicities of all the photons, while keeping their energies unchanged. If the multiplicities for the photons are assumed to vary with energy in accordance with the relation

$$M(E_n) = \frac{M_0 \left( E_n \sqrt{\frac{A+1}{A}} + Q \right)}{Q}$$

where  $M_0$  is the multiplicity for thermal neutrons, then the available energy will be conserved even though the cross sections for specific photons (and in particular the energies of the photon lines) will, in some cases, be incorrect.

For isotopes and elements with mass number greater than about 20, the gamma ray production cross sections associated with the  $(n, \gamma)$  reaction present an even more difficult problem in the sense that identification of photons with individual level transitions is usually not possible. For these materials, the photon lines measured at thermal neutron energies may be collected into energy "bins", and a more-or-less continuous spectrum fashioned from the available data. It is then usually assumed



(for lack of experimental information) that this normalized spectral shape remains constant, and the higher-energy  $(n, \gamma)$  cross section is taken to be the product of the  $(n, \gamma)$  cross section times the multiplicity corresponding to the incident neutron energy, where this multiplicity is the product of the measured thermal multiplicity times the increase in available energy, as shown above for  $\text{Be}^9$ .

For neutrons with energies greater than the  $(n, n'\gamma)$  threshold, there are in many cases measured photon production cross sections, including in some instances cascade photons from the low-lying levels. If these experimental data are available, they should certainly be used. If, on the other hand, no experimental data are available, then the formalism described in reference [26] can be used with some confidence from the threshold of the  $(nn'\gamma)$  reaction up to 20 MeV. This formalism, developed by Howerton and Plechaty [26] is based on the sharing of available energy between neutron-producing and gamma-ray-producing final state channels. The validity of the formalism was demonstrated recently by comparing calculated  $(n, \gamma)$  cross section values for tantalum with the detailed experimental data of reference [28]. For convenience, a short resumé of the Howerton-Plechaty formalism is presented here. The extension of this method to include the fission process is straightforward.

The Howerton-Plechaty formalism for calculating  $(n, \gamma)$  cross sections is based in part upon the observation that the experimental spectral data for photon production, when plotted as  $N(E_\gamma)/E_\gamma$  vs.  $E_\gamma$ , can be represented as straight lines on a semi-logarithmic plot. This leads to the relation

$$N(E_\gamma) = A E_\gamma \exp(-R(E_n)E_\gamma)$$

where A is a normalizing constant and

$$R(E_n) = - \frac{d \left[ \ln \left( \frac{N(E_\gamma)}{E_\gamma} \right) \right]}{dE_\gamma}$$

To obtain the normalizing constant A, we need to know, in addition to the spectral shape, the total energy available for photon emission. An average total photon energy  $\overline{E}_{TOT}$ , neglecting recoil, can be defined as

$$\overline{E_{TOT}} = \frac{\sum_{i=1}^3 (E_n - T_i - i \overline{E_i}) \sigma_{n,in}(E_n)}{\sum_{i=1}^3 \sigma_{n,in}(E_n)}$$

where  $\sigma_{n,in} = \sigma_{n,n'}$ ,  $\sigma_{n,2n}$  or  $\sigma_{n,3n}$  as  $i = 1, 2, 3$

$E_n$  = incident neutron energy,

$T_i$  = binding energy threshold for reaction  $i$ , and

$\overline{E_i}$  = average secondary neutron energy from reaction  $i$ .

Hence if we know the average neutron energy for each reaction  $i$ , then we also know the average gamma ray energy. By integrating the expression for  $N(E_\gamma)$  from  $E_{min}$  to  $\overline{E_{TOT}}$ , we have evaluated the normalizing constant  $\lambda$ . Since we know the gamma ray spectral shape and the total energy in the gamma ray spectrum, we can calculate the mean photon energy  $\overline{E_\gamma}$ . Then the photon multiplicity is given as

$$M_\gamma = \frac{\overline{E_{TOT}}}{\overline{E_\gamma}},$$

which leads to the expression for the  $(n, x\gamma)$  cross sections:

$$\sigma_{n,x\gamma} = M_\gamma \sum_{i=1}^3 \sigma_{n,in}$$

where the summation is over the available exit channels.

From this formalism, one can see that a dip will be observed in the  $(n, x\gamma)$  cross section at neutron energies just above the  $(n, 2n)$  threshold. The  $(n, 2n)$  cross section rises rapidly above threshold, reaching a value that is about 2/3 of the total nonelastic cross section at an energy of one to two MeV above the threshold. Thus the energy available for photons, and hence the photon production cross section, will decrease dramatically from the corresponding values immediately below the  $(n, 2n)$  threshold. This phenomenon is clearly observed in the data of reference [28]. As mentioned above, the formalism can easily be extended to include the fission process, and it can likewise be extended to charged particle reactions as well as  $(n, \gamma)$  reactions. The latter extension has been carried out and shows excellent agreement with experiment.

## VI.2. Approach by Fu and Perey [27]

A more detailed theoretical approach has been used in recent evaluations at the Oak Ridge National Laboratory. The two basic components of the theory are the "optical model" for neutron scattering [29] and the "statistical model" for decay of the compound nucleus [30]. The models and techniques involved in such calculations have now been developed and tested by many physicists over the past ten years, so that their reliability now justifies additional effort required for an evaluation of shielding material cross sections.

The initial step in this multistep process for generating gamma ray production cross sections involves the determination of parameters for the optical model description of the nucleus of interest. The optical model for nuclear scattering simply assumes that the target nucleus in a neutron-nucleus interaction can be replaced by a potential well. Then the quantum mechanical scattering equation is solved numerically for a range of incident neutron energies. The solution of the scattering problem yields the following energy dependent quantities:

- 1) Total cross sections
- 2) Shape elastic scattering cross sections
- 3) Angular distributions of shape-elastically scattered neutrons
- 4) Transmission coefficients
- 5) Neutron wave functions.

Comparison between measured and calculated cross sections and angular distributions are made and the model parameters adjusted until acceptable agreement is achieved. If the nucleus being studied is highly deformed like  $U^{238}$ , then it is possible to excite directly higher levels in the target nucleus. In a semi-classical sense one can picture the  $U^{238}$  nucleus as shaped like an egg. The neutron strikes the "egg" off-center and sets it rotating (e.g. the 45 kev  $2^+$  level). The result is direct inelastic neutron scattering. Such processes can be described by the distorted wave-Born approximation which requires the neutron wave functions as determined from the optical model as well as nuclear deformation parameters. The output will be

- 1) Inelastic neutron level excitation functions
- 2) Inelastic neutron angular distributions.

This direct reaction mechanism accounts for only a part of the inelastic cross section. In order to describe the remainder of the inelastic interaction as well as capture, fission, charged particle production, multiple neutron production, etc., one must employ compound nucleus theory [31]. Here one assumes that the incident neutron

is absorbed by the target nucleus forming an (A+1) nucleon system. This highly excited (A+1) nucleus decays according to the statistical probability of each energetically possible channel.

$$\sigma_{n,x} = \sigma_{CN} \frac{P_x}{\sum_i P_i}$$

where  $\sigma_{n,x}$  = cross section for reaction (n,x)

$\sigma_{CN}$  = cross section for compound nucleus formation

$P_x$  = probability of emission of particle x

$\sum_i$  is a sum over all competing reactions.

In the above equation all references to quantum number conservation laws have been suppressed for simplicity.

Optical model transmission coefficients determine the compound nucleus formation cross section. In addition one must supply nuclear structure data such as

- 1) Nuclear level schemes
- 2) Nuclear level densities
- 3) Reaction Q values
- 4) Optical model parameters for particle emission calculations
- 5) Fission barrier parameters
- 6) Average resonance capture parameters.

As output one obtains compound nucleus contributions to the elastic cross section and the inelastic excitation functions. These must be added to the corresponding optical model components. In addition one will get capture, fission, alpha emission, proton emission and other cross sections.

The cross sections calculated from optical model and compound nucleus theory must be compared with available experimental results. Thus one must iterate between steps one and two until satisfactory model parameters are developed. It is then possible to calculate the neutron cross sections for that nuclide on any desired energy grid.

A final step is necessary to generate gamma ray production cross sections. The gamma ray cascades from excited nuclei must be calculated. For example the (n, $\gamma$ ) reaction requires the calculation of the gamma ray

cascades generated during de-excitation of the  $(A+1)$  nucleon system. Usually a dipole model [ 32 ] is used in the region of compound nucleus excitation where the levels can be described by a level density. For lower excitation energies one must supply level structures and branching ratios. It is then possible to calculate gamma ray distributions and multiplicities.

This method has the advantage of requiring that all cross sections and spectra are self-consistent. This is necessary because no single reaction can be adequately evaluated without considering other competing reactions simultaneously. Secondly, the method will allow the gamma production cross sections for separate reactions to be calculated and not just a total gamma production cross section. However large amounts of nuclear structure data, cross section measurements, manpower and machine time are required to produce the evaluated data required.

In figure [ 12 ] are some typical results obtained by Fu and Perey for gamma production of discrete gamma rays from neutrons interacting with  $Pb^{206}$ . Figure [ 13 ] illustrates a typical gamma ray spectrum from inelastic scattering of 6.5 Mev neutrons on natural lead. Finally, figure [ 14 ] compares gamma production cross sections accompanying neutron emission with available experimental data.

## VII. The fission neutron spectrum

The knowledge of prompt fission neutron spectra is important as a neutron source in reactor shielding calculations. Shielding and core physics requirements for accuracy are the same for the lower energy part of the spectrum ( $< 5$  MeV). Neutrons of energies greater than 5 MeV form only a small part of the total number of neutrons produced in fission and so are rather unimportant for core physics calculations. However, for shielding applications this higher energy region is much more important as these are the neutrons most likely to leak out of a reactor core and blanket.

The simplest expression used to describe the fission neutron spectrum is the Maxwellian

$$N(E) \sim \sqrt{E} e^{-(E/T)}$$

where the average neutron energy  $\bar{E}$  is 1.5 times the temperature  $T$ . Most experimental determinations of the fission spectrum are analyzed in terms of this distribution. The mean of 9 measurements for the average energy of the fission spectrum of  $U^{235}$  is  $1.979 \pm .086$  MeV and for  $Pu^{239}$  the average is  $2.084 \pm .050$  MeV [ 33 ].

However, it is clear from all available spectrum measurements that the Maxwellian distribution is inadequate to describe the fission neutron spectrum over the entire energy range. If a Maxwellian is fitted to the low energy part of the neutron spectrum, then for  $U^{235}$  the data begin to deviate systematically from a Maxwellian shape at about 4 MeV. In most cases the Watt spectrum gives a better fit to the data:

$$N(E) \sim e^{-bE} \sinh \sqrt{cE}$$

The difference between the two representations is about 5% at 6 MeV and 25% at 10 MeV. There are also indications from experimental data that there are more low energy neutrons than predicted by either expression. This point was discussed at the recent IAEA Consultants Meeting on Fission Neutron Spectra [ 33 ] with the result that it can not be excluded that this is due to scattering and consequent slowing down of fission neutrons.

An important aspect of the description of the prompt fission neutron energy spectrum often neglected is its dependence on incident neutron energy. Terrell [ 34 ] derived the following relation for the mean spectrum energy:

$$\bar{E} = A + B\sqrt{\bar{\nu} + 1} \quad [\text{MeV}]$$

where  $\bar{\nu}(E)$  = average number of neutrons per fission

$$A = 0.75 \text{ MeV}$$

$$B = 0.65 \text{ MeV}$$

Thus an incident energy dependence of the fission neutron spectrum is implied through the energy dependence of  $\bar{\nu}$ . Howerton and Doyas [35] point out that the Terrell expression applies only to the (n,f) process. Above the threshold for  $\sigma_{n,n'f}$  and  $\sigma_{n,2nf}$  the following should be used

$$\bar{\nu}_f(E) = \frac{\bar{\nu}_T(E) \sigma_f(E) - \sigma_{n,n'f}(E) - 2\sigma_{n,2nf}(E)}{\sigma_f(E)}$$

where  $\bar{\nu}_f$  is the effective  $\bar{\nu}$  to be used in the Terrell expression. By a least squares update of the constants A and B from recent  $\bar{\nu}$  data Howerton and Doyas [35] got

$$A = 0.530 \text{ MeV and}$$

$$B = 0.765 \text{ MeV.}$$

However, not all the available data are consistent with this expression. Major work in this area seems still to be needed.

The present uncertainties in the knowledge of the fission neutron spectrum result partly from discrepancies between microscopic and macroscopic measurements. By microscopic measurements, the energy differential measurements of fission neutron spectra are meant; macroscopic measurements include all measurements of the type

$$\int \sigma(E) \sqrt{E} N(E) dE$$

where  $\sigma(E)$  is some energy dependent cross section

and  $N(E)$  is the fission neutron spectrum.

Results of some macroscopic measurements, most typically by activation analysis, imply a mean fission energy of ~2.2 MeV, well outside the confidence limit of the microscopic measurements. Work reported by Grundl [36] used a cavity containing the fissionable material and a detector surrounded by  $D_2O$ . The analysis of the activation data for several detector materials in fission neutron spectra of  $U^{233}$ ,  $U^{235}$  and  $Pu^{239}$  indicated a 20% "depletion" of neutrons below 1.4 MeV and a 30%

"bulge" in the region 3-5 MeV as compared to a Maxwellian with an average energy of 1.9 to 2.0 MeV. McElroy [ 37 ] analyzed an extensive set of activation measurements in a  $U^{235}$  fission neutron spectrum and concluded that the average fission energy was  $\sim 2.2$  MeV.

The analysis of activation measurements is complicated by several factors including the 20-25% discrepancies between reported directly measured fission spectrum average activation cross sections, the 15-20% uncertainty in the energy dependent activation cross sections and the corrections for absorption and scattering which are needed as the flux seen by the foils differs from a virgin fission flux, and finally the inherent instability and lack of uniqueness in "unfolding" techniques.

Analyses of a series of fast critical experiments by Campbell and Rowlands [ 38 ] suggest that the mean energy of the fission neutron spectrum may be 5-10% higher than 2.0 MeV. Similar uncertainties were reported by Okrent et al. [ 39 ] for ZEBRA-2 and LFR-2 critical assemblies. On the other hand the results of comparing measured and calculated leakage spectra from fast critical assemblies like Godiva ( $U^{235}$ ) and Jezebel ( $Pu^{239}$ ) indicate a good consistency with the microscopic measurements of the fission neutron spectrum.

Finally there are measurements of the neutron age in moderator materials which are extremely sensitive to the mean energy of the fission spectrum. Excellent agreement is obtained between the best value of the neutron age in  $H_2O$  and Monte Carlo calculations using a fission spectrum mean energy of  $\sim 1.98$  MeV [ 40 ].

In summary, it seems difficult to believe that the fission neutron spectrum is the cause of the current discrepancies between microscopic and macroscopic determinations of that quantity at this time. Considerable refinement in the activation techniques would be necessary before more definite conclusions can be reached.



Acknowledgements

The authors wish to acknowledge valuable contributions to this paper made by J. Butler, R. Roussin and J.S. Story. They also gratefully acknowledge the information supplied by T.A. Byer, G. Hehn, R. Meyer, F.G. Perey and H. Vossebrecker.

## References

1. H. Goldstein, First IAEA Conference on Nuclear Data for Reactors, Paris, 1966, Proceed. Vol. I, p.39 ff.
2. H. Goldstein, Second Conf. on Neutron Cross Sections and Technology, Washington, March 1968, Proceed. Vol.I, p.37 ff.
3. "The Physics Problems of Reactor Shielding", Report of a Joint ENEA/IAEA Specialists Meeting, Paris, December 1970, Proceedings edited by the OECD, Summary report, p.9 ff.
4. H. Goldstein et al., Third Conf. on Neutron Cross Sections and Technology, Knoxville, Tennessee, March 1971, Proceed. Vol.I, p.106 ff.
5. RENDATA 72, "A world-wide Compilation of Requests for Neutron Data Measurements for Reactors", INDC(SEC)-27/L, October 1972
6. F.H. Fröhner, S. Valente, "On Shielding Calculations with Computer Files of Neutron Data", paper presented at this Conference
7. J. Butler, private communication, 1972
8. H. Vossebrecker, private communication, 1972
9. National Neutron Cross Section Center (NNCSC) Newsletters, Brookhaven National Laboratory
10. CCDN Newsletter/Bulletin CCDN-NW/13, February 1972
11. IAEA Report CINDU-10, May 1972
12. O.D. Simpson et al., EANDC Symposium on Neutron Standards and Flux Normalization, Argonne National Laboratory, 1971, page 362
13. J.A. Harvey, private communication
14. H. Goldstein et al., paper presented at this Conference
15. G. Hehn, private communication, 1972
16. B.F. Maskewitz et al., paper presented at this Conference
17. R.W. Roussin et al., paper presented at this Conference
18. B. Hinkelmann et al., KFK 1340, 1971
19. Proceed. of the IAEA Panel on Neutron Nuclear Data Evaluation, Vienna, August/September 1971, to be published
20. D. Woll, KFK 880, 1968
21. J.K. Dickens et al., ORNL-TM-3850, 1972
22. J.K. Dickens and F.G. Perey, Nucl. Sci. Eng. 36, 280, 1969

23. C. Wong, J.D. Anderson, P. Brown, L.F. Hansen, J.L. Kammerdiener, C. Logan, and B. Pohl, "Livermore Pulsed Sphere Program: Program Summary Through July 1971", Report UCRL-51144, Rev.1, Lawrence Livermore Laboratory, Livermore, California, 1972
24. D.M. Drake et al., Nucl. Sci. Eng. 40,294,1970
25. V.J. Orphan et al., Proceedings of the Third Conference on Neutron Cross Sections and Technology, Knoxville, Tennessee, March 1971, CONF-710301, Vol.1, p.227 ff.; see also V.J. Orphan et al., Gulf Radiation Technology Report RT-A10743, June 1971
26. R.J. Howerton and E.F. Plechaty, Nucl. Sci. Eng. 32,178,1968
27. C.Y. Fu and F.G. Perey, Report ORNL-4765, Oak Ridge National Laboratory, Oak Ridge, Tennessee, 1972
28. D.L. Morgan, T.A. Love, J.K. Dickens and F.G. Perey, Report ORNL-TM-3702, Oak Ridge National Laboratory, Oak Ridge, Tennessee,1972
29. H. Feshbach, C.E. Porter and V.F. Weisskopf, Phys. Rev. 96,488,1954
30. W. Hauser and H. Feshbach, Phys. Rev. 87,366,1952
31. C.L. Dunford, Report AI-AEC-12931, Atomics International, Canoga Park, California, 1970
32. E.S. Troubetzkoy, Phys. Rev. 122,212,1961
33. A.B. Smith, IAEA Consultants Meeting on the Status of Prompt Fission Neutron Spectra, August 1971, Proceedings to be published
34. J. Terrell, Phys. Rev. 113,527,1959; J. Terrell, IAEA Symposium on the Physics and Chemistry of Fission, Salzburg, 1965, Proceed. Vol.II, p.3 ff.
35. R.J. Howerton and R.J. Doyas, Nucl. Sci. Eng. 46,419,1971
36. J.A. Grundl, Nucl. Sci. Eng. 31,191,1968
37. W.N. McElroy, Nucl. Sci. Eng. 36,109,1969
38. C. Campbell and J. Rowlands, Second IAEA Conference on Nuclear Data for Reactors, Helsinki 1970, Proceed. Vol.II, p.391 ff.
39. D. Okrent et al., Nucl. Applications and Tech. 9,454,1970
40. C. Dunford and H. Alter, AI-AEC-MEMO-12915, 1971

Figure 1. Nuclear data requests for shielding

Extract from RENDA 72

Requested quantity	Element or isotope	Energy range	Accuracy (%)		No. of requests	Priority	Average priority	Requesting countries or organisations
			range	average				
$\sigma_{n,T}(E)$	Na	10 KeV-5 MeV	1	1	1	1	1	USA
	Ni	0.3-3.2 MeV	1	1	1	2	2	USA
$\sigma_{n,n}(E, \Theta)$	C, O, Na, Al, Si, Ca, Cr, Fe, Ni	mostly MeV range	5-20	12	1 8 2	1 2 3	2.1	France, FRG, South Africa, Sweden, UK, USA
	C, Na, Al, Ca, Cr, Fe, Nb, Ba, W	threshold -16 MeV	5-20	10	1 2 7	1 2 3	2.6	Belgium, C.E.C. (EURATOM), France, South Africa, UK
	Be, Ti, V, Fe, Ni, Nb, Mo	threshold -15 MeV	15	15	7	3	3	Belgium, C.E.C. (EURATOM)
$\sigma_{n,n'}(E, E', \Theta)$	O, Al, Si, Cr, Fe, Ni, W, Pb	0.5-16 MeV	5-15	10	2 12 1	1 2 3	1.9	France, Sweden, USA
	O, Al, Si, Ca, Cr, Fe, Ni, W, Pb, Th-232, U-238	0.004 eV -16 MeV	10-20	15	3 17	1 2	1.9	France, South Africa, USA

Figure 2

 $\sigma_{n,T}$ 

~~ENDF~~

UKNDL

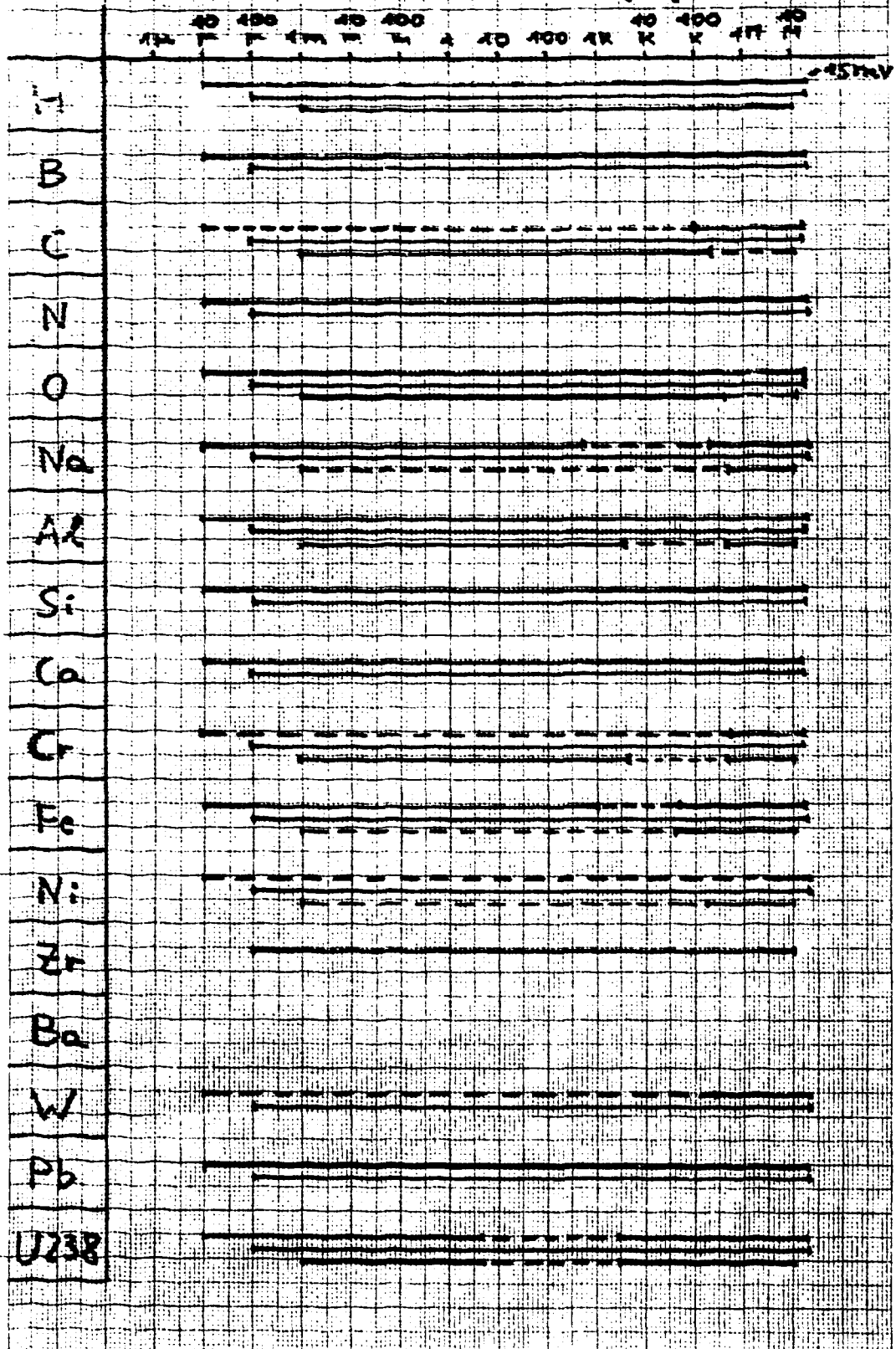
**KEDAK**

dashed line:

range of fi-

VERE VERBODEN

parameters

$$\rightarrow \pi(e\nu)$$


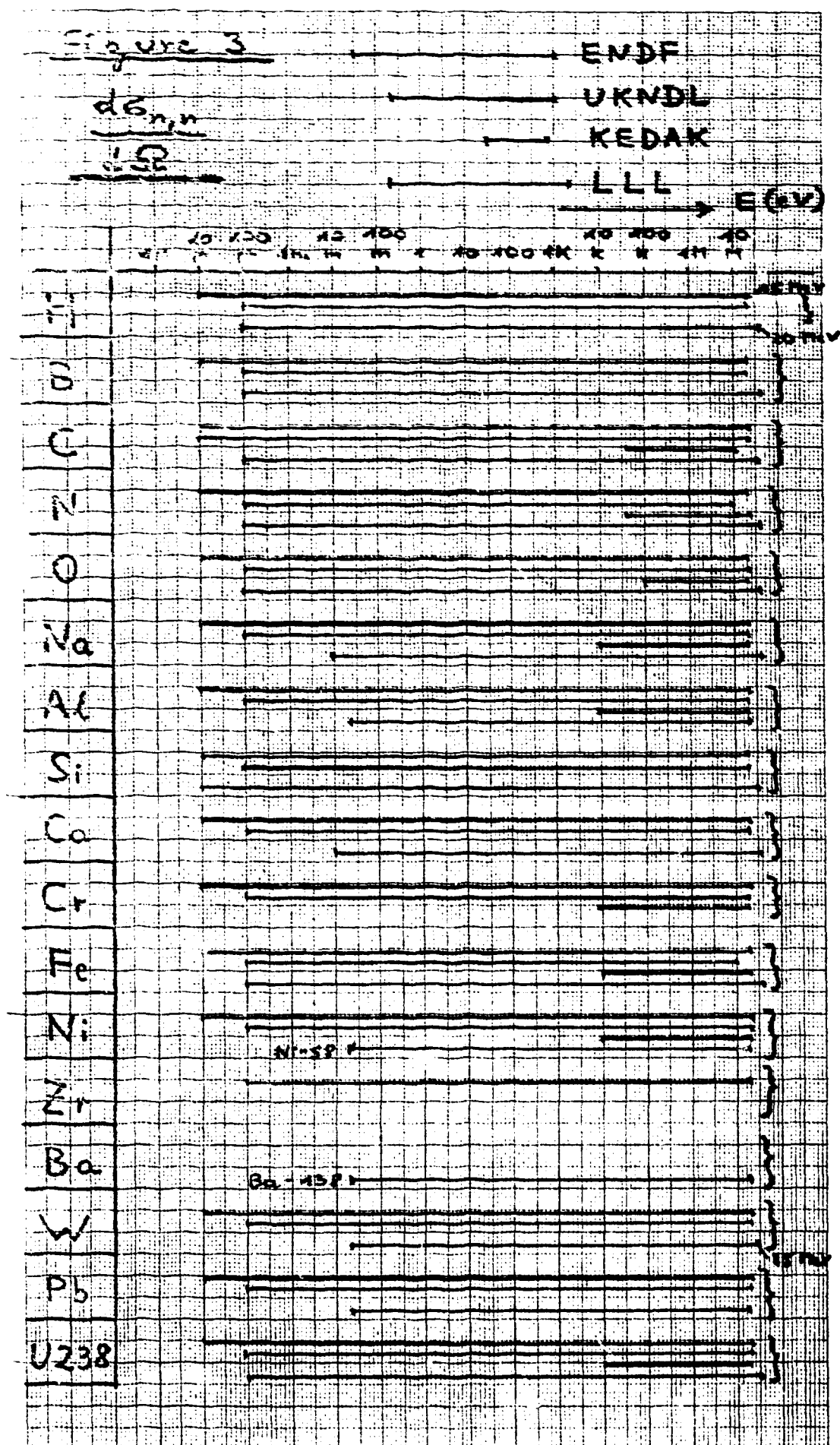
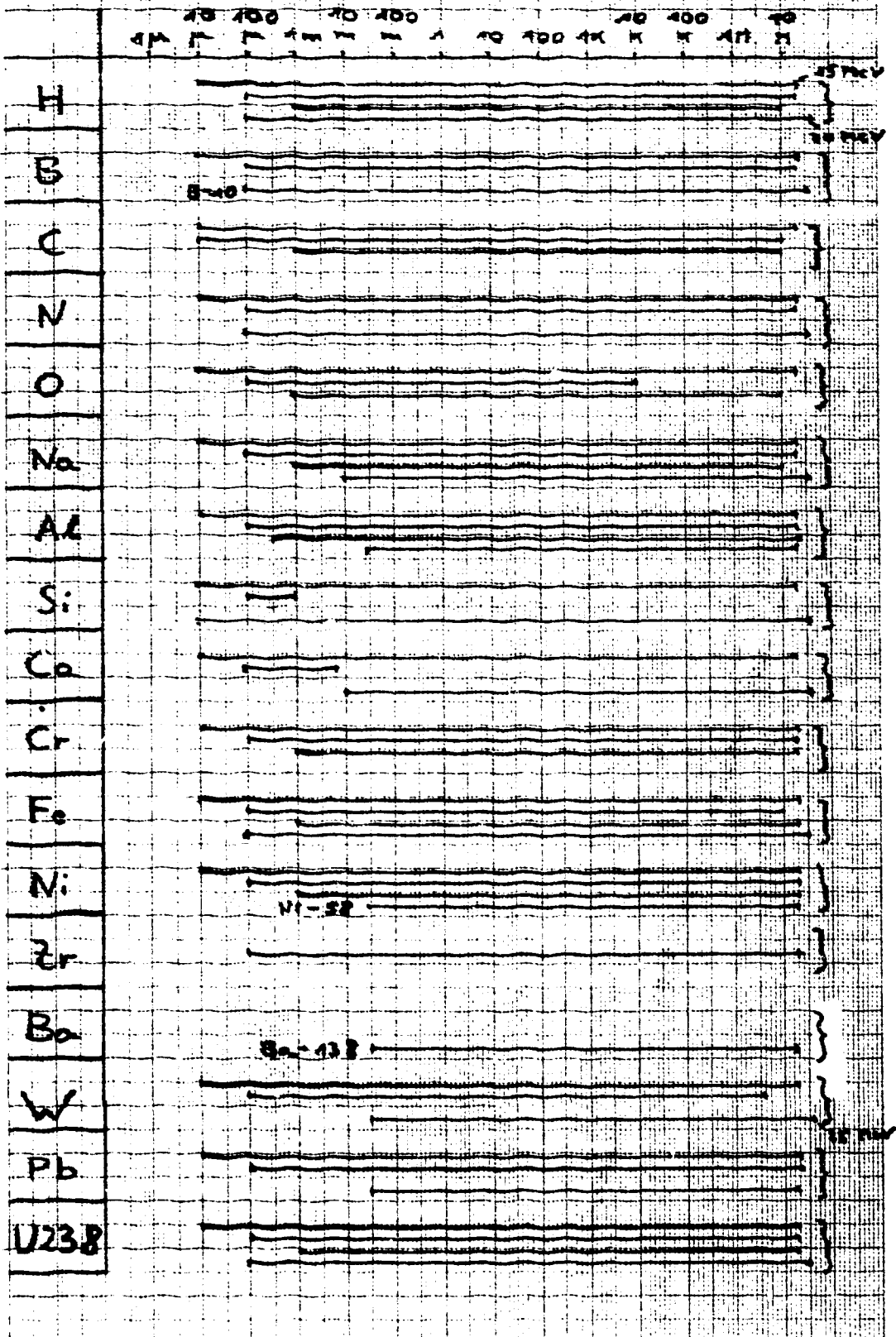


Figure 4

$\sigma_{n,\gamma}$

ENDF  
UKNDL  
KEDAK  
LLL

$\rightarrow E(\text{eV})$







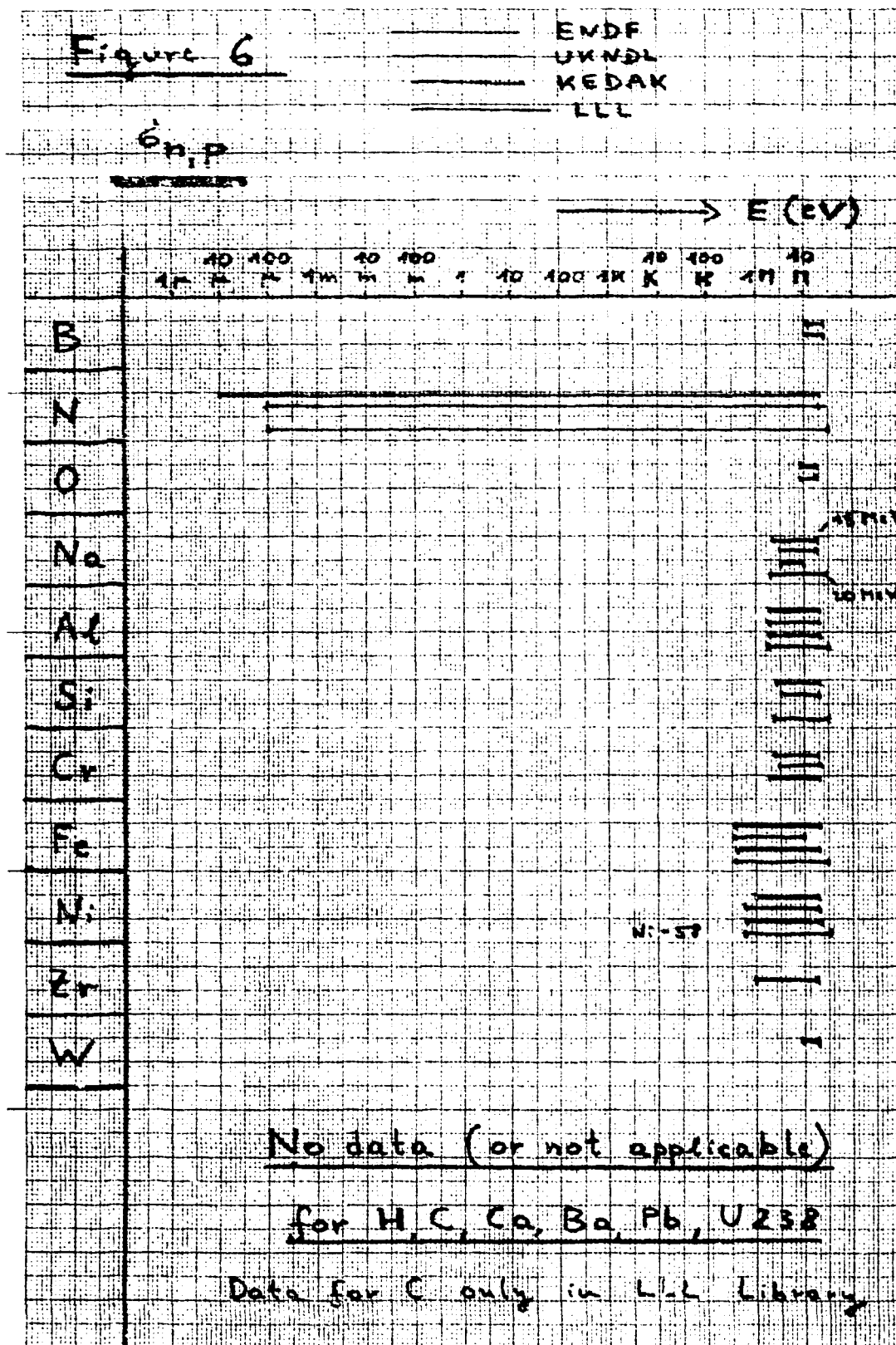


Figure 7

Content of major evaluated nuclear data libraries with regard to

neutron and gamma production cross sections

$E_i$  = level energy

Quantity	H	B	C	N	O	Na	Al	Si	Ca
$\sigma_{n,n'}(E, E_i)$		$\sigma_{n,n'}(E, E_i)$ B <sub>10,n</sub>	$\sigma_{n,n'}(E, E_i)$ C <sub>12,n</sub>	$\sigma_{n,n'}(E, E_i)$ N <sub>14,n</sub>	$\sigma_{n,n'}(E, E_i)$ O <sub>16,n</sub>	$\sigma_{n,n'}(E, E_i)$ Na <sub>23,n</sub>	$\sigma_{n,n'}(E, E_i)$ Al <sub>27,n</sub>	$\sigma_{n,n'}(E, E_i)$ Si <sub>28,n</sub>	$\sigma_{n,n'}(E, E_i)$ Ca <sub>40,n</sub>
$\sigma_{n,n'}(E, E_\gamma)$		$\sigma_{n,n'}(E, E_\gamma)$ B <sub>10,n</sub>	$\sigma_{n,n'}(E, E_\gamma)$ C <sub>12,n</sub>	$\sigma_{n,n'}(E, E_\gamma)$ N <sub>14,n</sub>	$\sigma_{n,n'}(E, E_\gamma)$ O <sub>16,n</sub>	$\sigma_{n,n'}(E, E_\gamma)$ Na <sub>23,n</sub>	$\sigma_{n,n'}(E, E_\gamma)$ Al <sub>27,n</sub>	$\sigma_{n,n'}(E, E_\gamma)$ Si <sub>28,n</sub>	$\sigma_{n,n'}(E, E_\gamma)$ Ca <sub>40,n</sub>
$\sigma_{n,n'}(E, E_\gamma, \Theta)$		$\sigma_{n,n'}(E, E_\gamma, \Theta)$ B <sub>10,n</sub>	$\sigma_{n,n'}(E, E_\gamma, \Theta)$ C <sub>12,n</sub>	$\sigma_{n,n'}(E, E_\gamma, \Theta)$ N <sub>14,n</sub>	$\sigma_{n,n'}(E, E_\gamma, \Theta)$ O <sub>16,n</sub>	$\sigma_{n,n'}(E, E_\gamma, \Theta)$ Na <sub>23,n</sub>	$\sigma_{n,n'}(E, E_\gamma, \Theta)$ Al <sub>27,n</sub>	$\sigma_{n,n'}(E, E_\gamma, \Theta)$ Si <sub>28,n</sub>	$\sigma_{n,n'}(E, E_\gamma, \Theta)$ Ca <sub>40,n</sub>
$\sigma_{n,n'}(E, E'_i, \Theta)$		$\sigma_{n,n'}(E, E'_i, \Theta)$ B <sub>10,n</sub>	$\sigma_{n,n'}(E, E'_i, \Theta)$ C <sub>12,n</sub>	$\sigma_{n,n'}(E, E'_i, \Theta)$ N <sub>14,n</sub>	$\sigma_{n,n'}(E, E'_i, \Theta)$ O <sub>16,n</sub>	$\sigma_{n,n'}(E, E'_i, \Theta)$ Na <sub>23,n</sub>	$\sigma_{n,n'}(E, E'_i, \Theta)$ Al <sub>27,n</sub>	$\sigma_{n,n'}(E, E'_i, \Theta)$ Si <sub>28,n</sub>	$\sigma_{n,n'}(E, E'_i, \Theta)$ Ca <sub>40,n</sub>
$\sigma_{2n}(E, E_i)$		$\sigma_{2n}(E, E_i)$ B <sub>10,n</sub>	$\sigma_{2n}(E, E_i)$ C <sub>12,n</sub>	$\sigma_{2n}(E, E_i)$ N <sub>14,n</sub>	$\sigma_{2n}(E, E_i)$ O <sub>16,n</sub>	$\sigma_{2n}(E, E_i)$ Na <sub>23,n</sub>	$\sigma_{2n}(E, E_i)$ Al <sub>27,n</sub>	$\sigma_{2n}(E, E_i)$ Si <sub>28,n</sub>	$\sigma_{2n}(E, E_i)$ Ca <sub>40,n</sub>
$\sigma_{2n}(E, E'_i, \Theta)$		$\sigma_{2n}(E, E'_i, \Theta)$ B <sub>10,n</sub>	$\sigma_{2n}(E, E'_i, \Theta)$ C <sub>12,n</sub>	$\sigma_{2n}(E, E'_i, \Theta)$ N <sub>14,n</sub>	$\sigma_{2n}(E, E'_i, \Theta)$ O <sub>16,n</sub>	$\sigma_{2n}(E, E'_i, \Theta)$ Na <sub>23,n</sub>	$\sigma_{2n}(E, E'_i, \Theta)$ Al <sub>27,n</sub>	$\sigma_{2n}(E, E'_i, \Theta)$ Si <sub>28,n</sub>	$\sigma_{2n}(E, E'_i, \Theta)$ Ca <sub>40,n</sub>
$\sigma_{2n}(E, E_\gamma)$		$\sigma_{2n}(E, E_\gamma)$ B <sub>10,n</sub>	$\sigma_{2n}(E, E_\gamma)$ C <sub>12,n</sub>	$\sigma_{2n}(E, E_\gamma)$ N <sub>14,n</sub>	$\sigma_{2n}(E, E_\gamma)$ O <sub>16,n</sub>	$\sigma_{2n}(E, E_\gamma)$ Na <sub>23,n</sub>	$\sigma_{2n}(E, E_\gamma)$ Al <sub>27,n</sub>	$\sigma_{2n}(E, E_\gamma)$ Si <sub>28,n</sub>	$\sigma_{2n}(E, E_\gamma)$ Ca <sub>40,n</sub>

Figure 7 continued

Quantity	Cr	Fe	Ni	Zr	Ba	W	Pb	U238
$\sigma_{n,n'}(E, E_i)$	OX ● □ OX ● □ OX ● □ OX	OX ● □ OX ● □ OX ● □ OX	OX ● □ OX ● □ OX ● □ OX	OX ● □ OX ● □ OX ● □ OX	OX ● □ OX ● □ OX ● □ OX	OX ● □ OX ● □ OX ● □ OX	OX ● □ OX ● □ OX ● □ OX	OX ● □ OX ● □ OX ● □ OX
$\sigma_{n,n'}(E, E_\gamma)$	●	●	●	●	● Ba-138	●	●	●
$\sigma_{n,n'}(E, E_\gamma, \ominus)$								●
$\sigma_{n,n'}(E, E', \ominus)$	OX	OX	OX	OX Zr-95	OX	OX stable isotopes	OX	OX
$\sigma_{2n}(E, E')$		●	● Ni-58		● Ba-137	● -13n	●	● -13n +3n +4n
$\sigma_{2n}(E, E', \ominus)$	OX	OX	OX	X		OX	OX -1 +3n	OX -1 +3n
$\sigma_{2n}(E, E_\gamma)$								

Fig. 8. Gamma-ray spectrum for the  $\text{Fe}(n, \gamma)$  reaction at  $E_n = 4.85$  MeV,  $\theta_\gamma = 125^\circ$ . Each whole segment has 750 channels. Peaks corresponding to transitions in  $^{56}\text{Fe}$  are indicated by the larger labels. Peaks known to be due to other nuclei are indicated by isotope symbol. Full energy peaks are labelled with the gamma-ray energy; escape peaks are labelled with  $(E_\gamma - 511)$  and  $(E_\gamma - 1022)$  for the single- and double-escape modes, respectively.

(taken from reference [21])

ORNL-DWG 72-977R

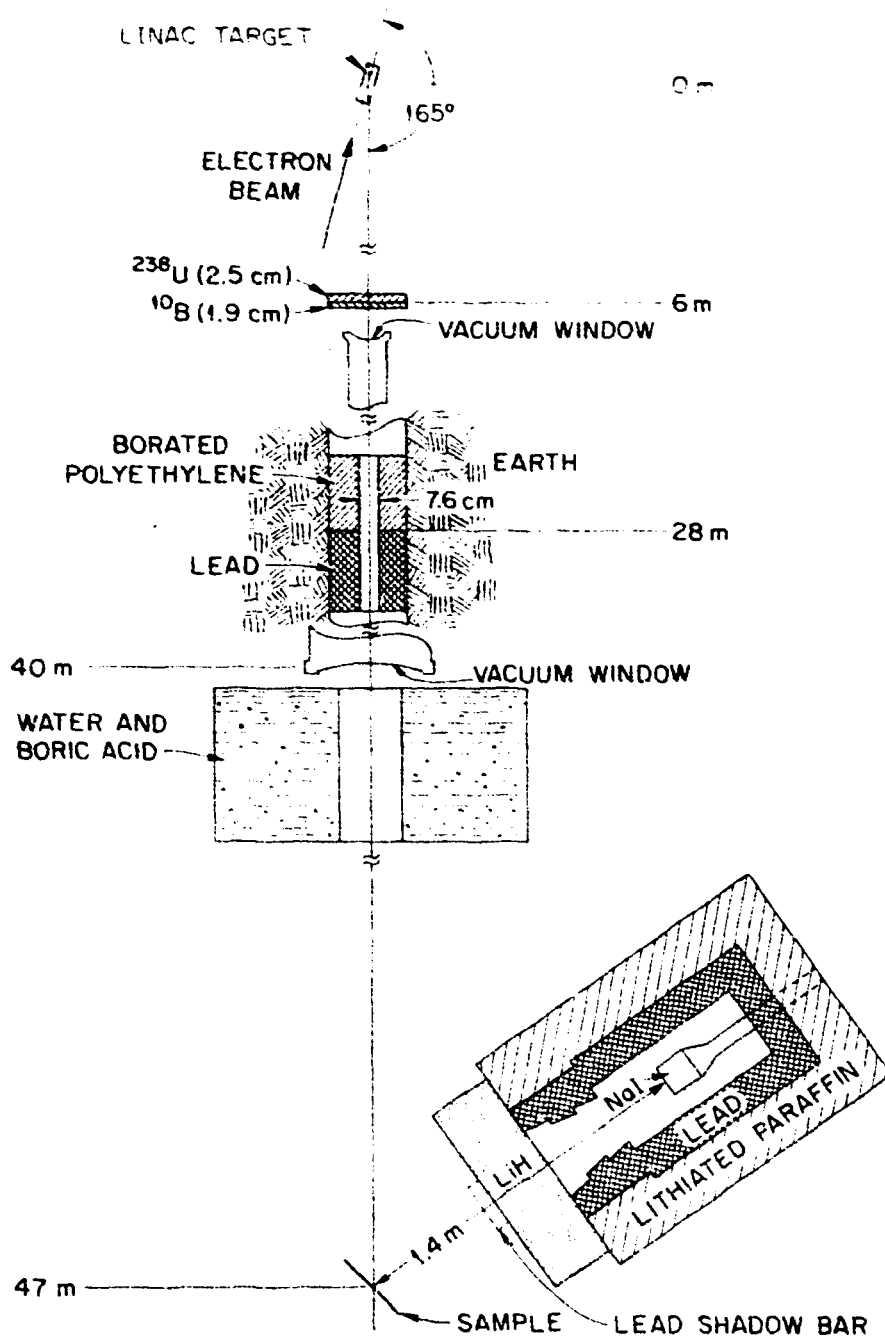


Fig. 9. Experimental arrangement showing neutron source, flight path with collimators and filters, and NaI spectrometer. The shadow bar shown dotted is used for background measurements.

(taken from reference [21])

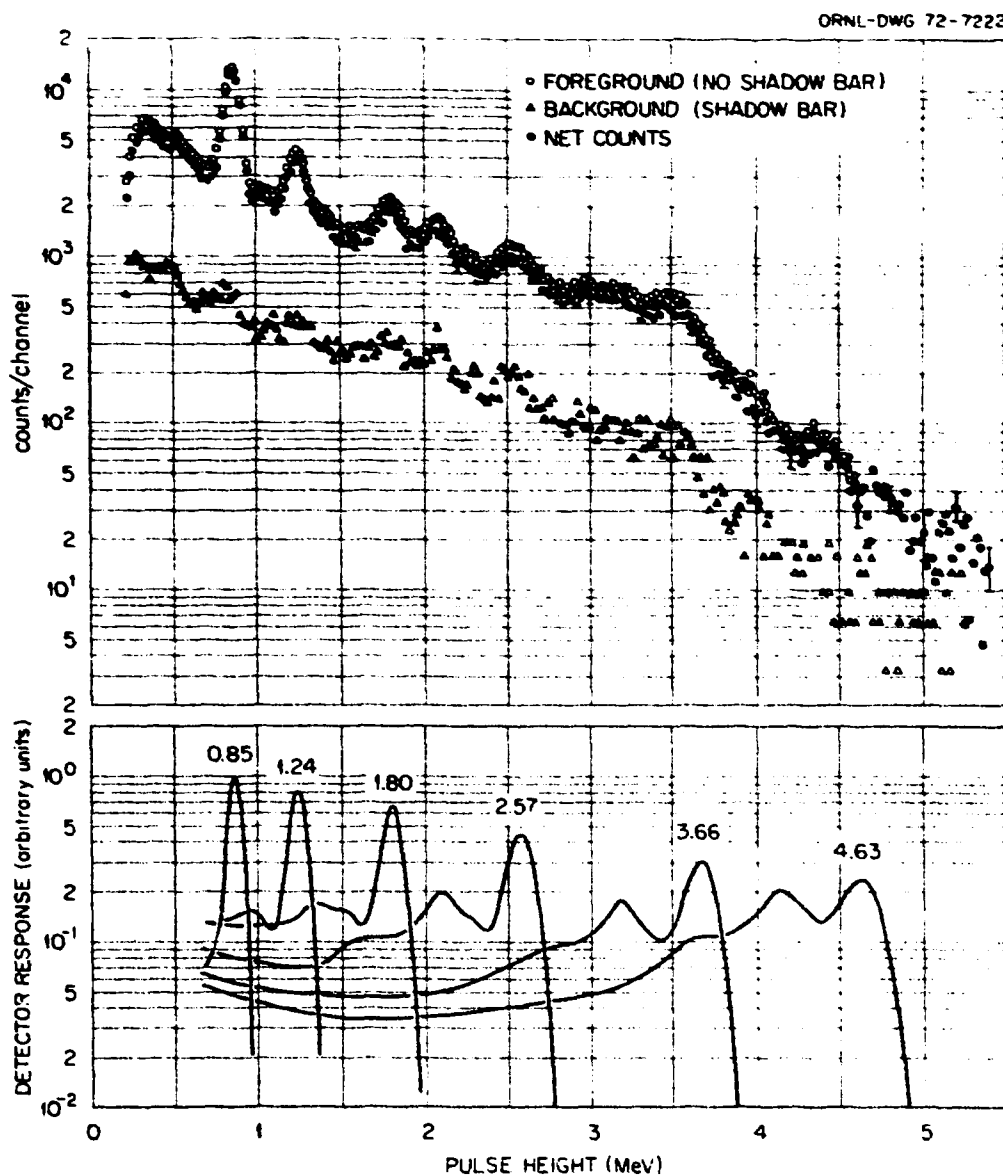


Fig. 1C. Gamma-ray pulse-height spectra produced by 5.14 to 6.13 MeV neutron interactions with iron. The background spectrum obtained by placing the 5.1 cm lead shadow bar in front of the collimator. The curves shown at the bottom of figure are some of the response functions for the NaI detector.

(taken from reference [21])

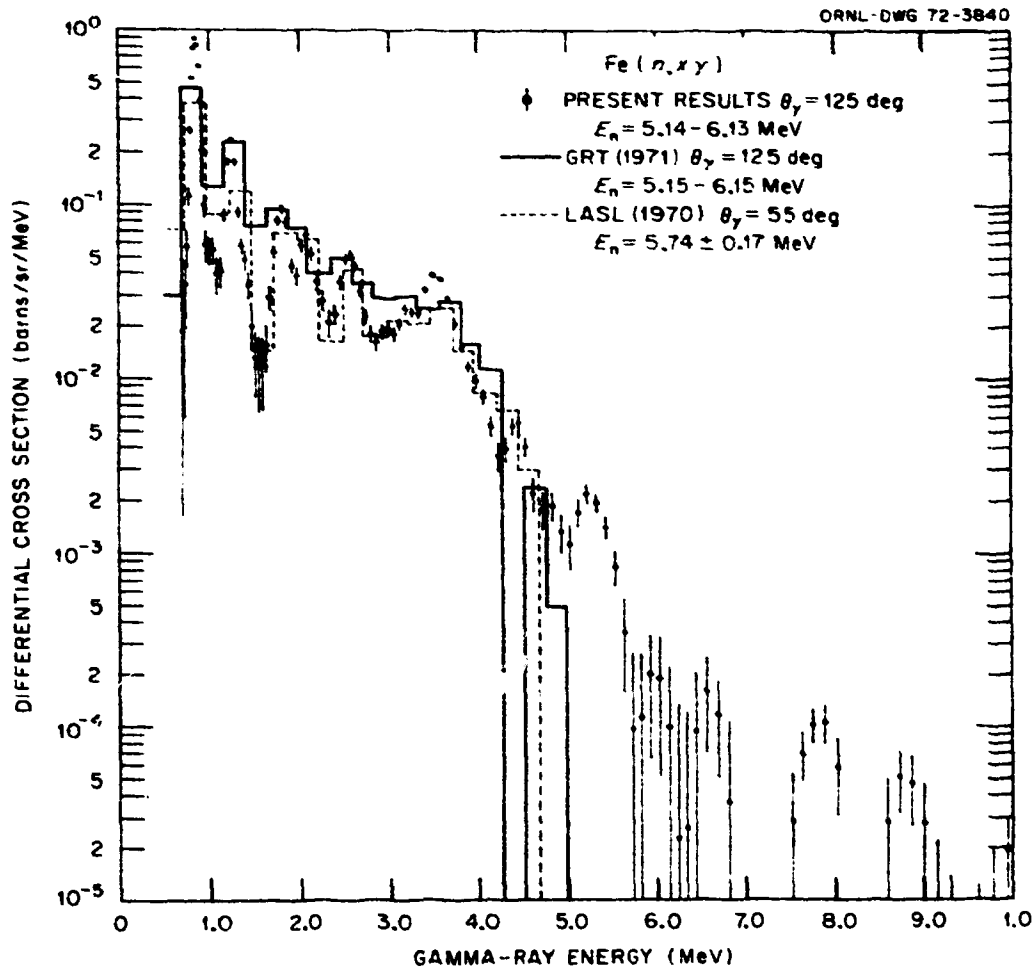


Fig. 11. Differential cross sections for gamma rays produced by 5.14- to 6.13-MeV neutron interactions with iron. The present results are compared with similar data reported by Drake et al., (LASL (Ref. 3) and Orphan et al., GRT (Ref. 6).

(taken from reference [21])

ORNL-DWG 71-10940

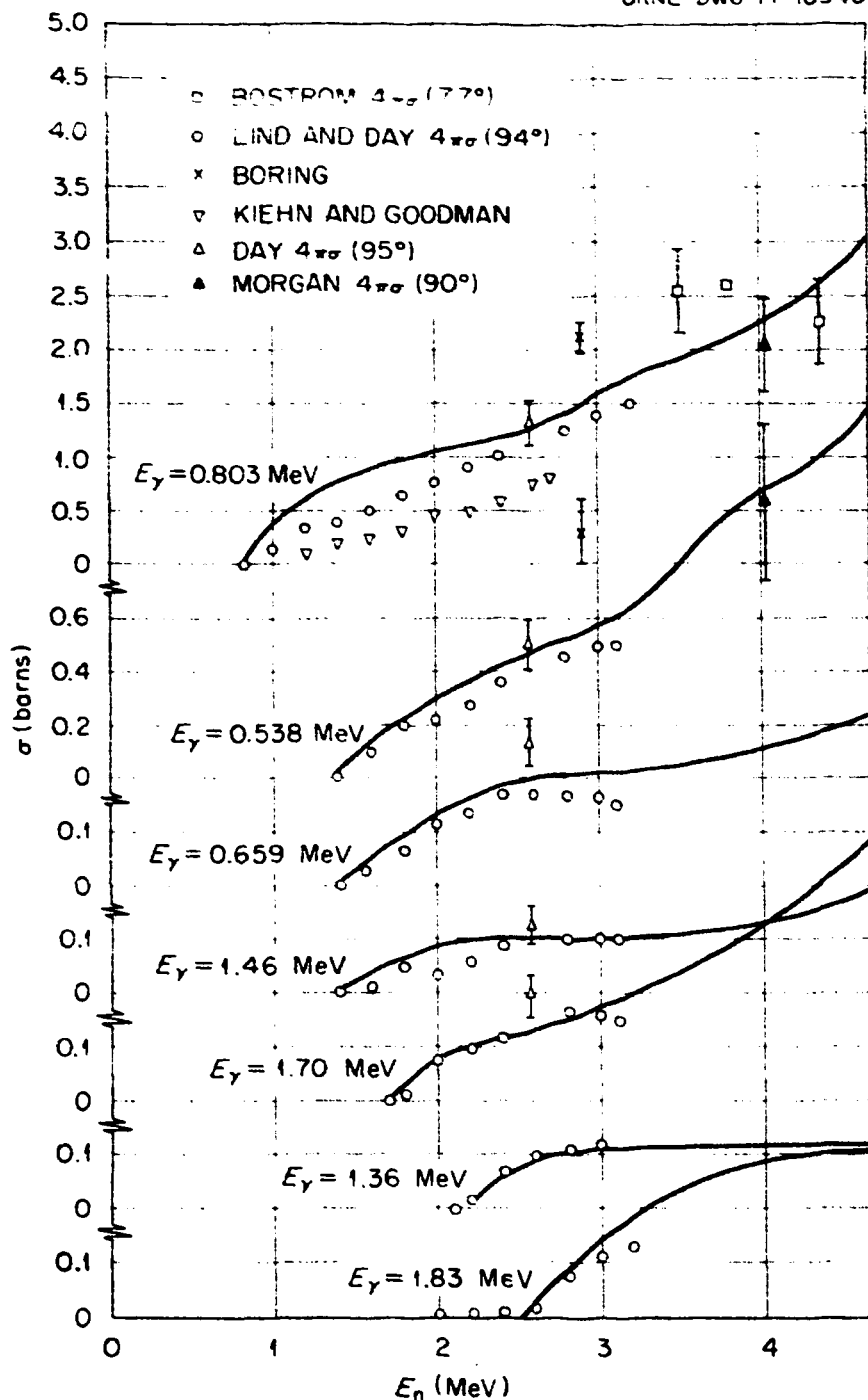


Fig. 12. Comparison of calculation with experiment for the production cross sections of discrete gamma rays in  $^{206}\text{Pb}$ .

(taken from reference [27])



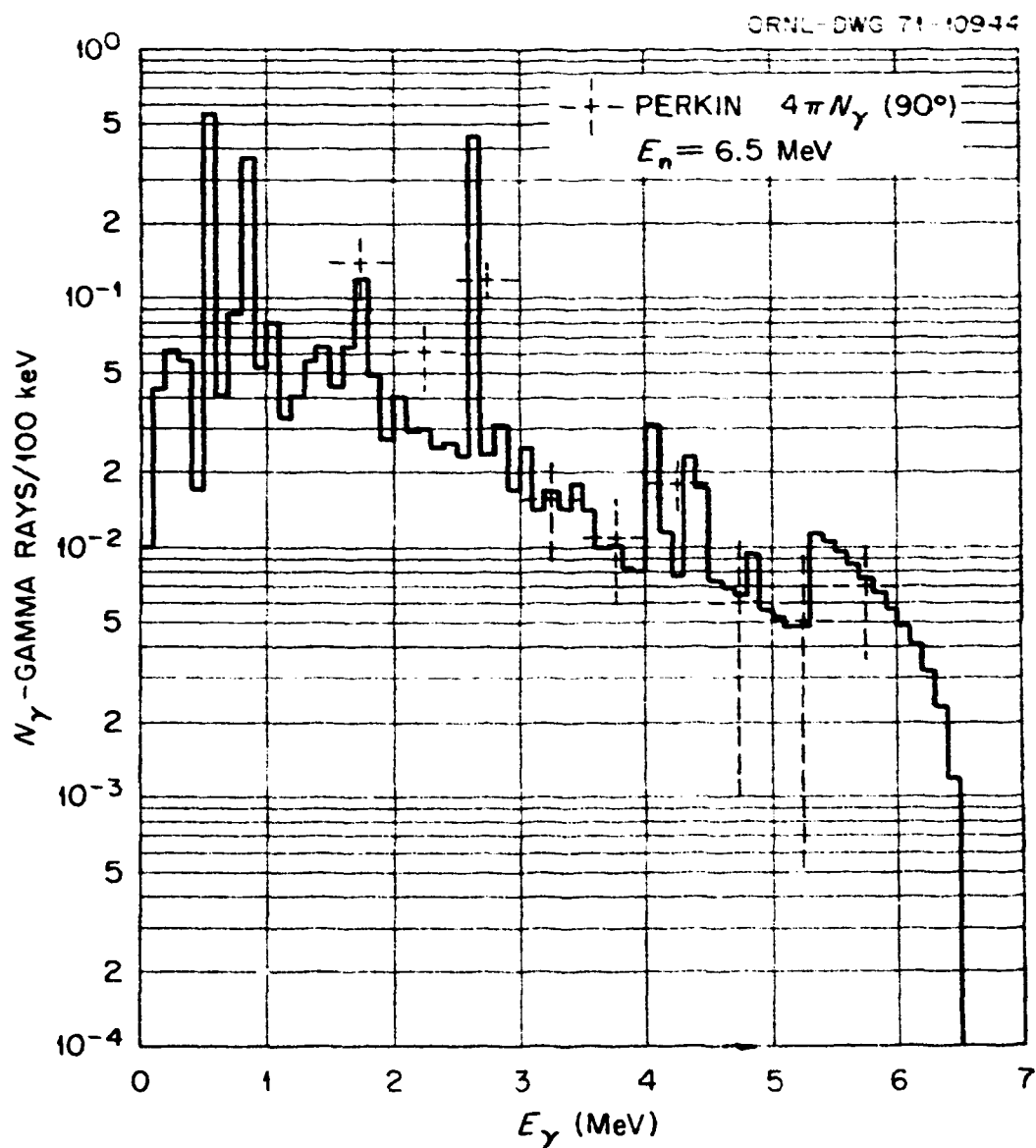


Fig. 13. Comparison of calculation with experiment for the gamma-ray yield spectrum from inelastic scattering of 6.5 MeV neutrons with natural lead.

(taken from reference [27])

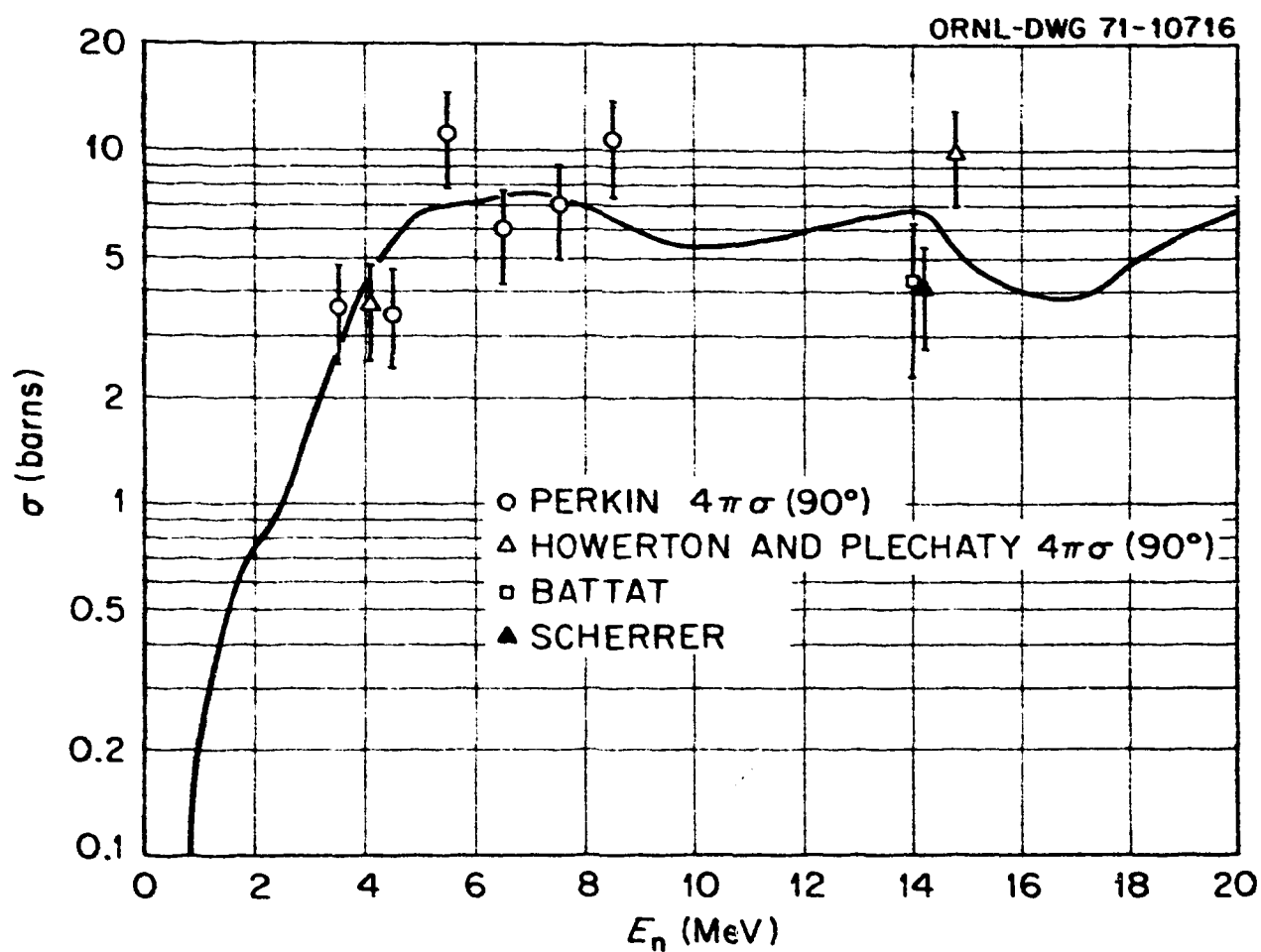


Fig. 14. Comparison of calculation with experiment for the total gamma-ray production cross sections for the sum of  $(n,n')$ ,  $(n,2n)$ , and  $(n,3n)$  reactions.

(taken from reference [27])